Materials Science in Semiconductor Processing ▮ (▮▮▮▮) ▮▮▮–▮▮▮

Contents lists available at ScienceDirect

Materials Science in Semiconductor Processing

journal homepage: www.elsevier.com/locate/mssp

Parametric optimization of mechanochemical process for synthesis of $Cu(In, Ga)_{0.5}Se_2$ nanoparticles

M. Rohini [a], P. Reyes [a], S. Velumani [a,b,*], M. Latha [b], Goldie oza [a], I. Becerril-Juarez [b], R. Asomoza [a]

[a] Department of Electrical Engineering (SEES), CINVESTAV-IPN, Avenida IPN 2508, San Pedro Zacatenco, Mexico D.F, Mexico
[b] Program on Nanoscience and Nanotechnology, CINVESTAV-IPN, Avenida IPN 2508, San Pedro Zacatenco, Mexico D.F, Mexico

ARTICLE INFO

Keywords:
Mechanochemical synthesis
Ball to powder ratio
Milling time and milling speed

ABSTRACT

Copper indium gallium diselenide (CIGS) is a promising photovoltaic material. Non-vacuum deposition of CIGS is a recommended strategy to produce cost effective solar cells. Amongst various non-vacuum deposition techniques, nanoparticle based deposition methods have gained major impetus due to their economic benefits, simplicity and flexibility to scale up. In the present work, CIGS nanoparticles are synthesized by a mechanochemical process and the effect of milling parameters (ball to powder ratio (BPR), milling speed (rpm) and milling time) on the structural, morphological and compositional properties have been studied. CIGS nanoparticles are synthesized with BPR of 15:1, 20:1 and 25:1 for different milling times ranging from 1 to 6 h and milling speeds from 200 to 400 rpm. The synthesized CIGS nanoparticles have been characterized using XRD, FESEM, HRTEM and EDAX analysis. XRD analysis showed the formation of chalcopyrite CIGS nanoparticles without any secondary phase within 2 h of milling time with a BPR of 25:1 at 400 rpm. The influence of milling parameters on morphology and agglomeration has been studied using FESEM. It is observed that the nanoparticles synthesized at higher BPR with shorter milling time, are less agglomerated. The compositional study performed by EDAX analysis showed that the synthesized CIGS nanoparticles are in good match with the desired stoichiometry of $Cu(In,Ga)_{0.5}Se_2$.

1. Introduction

The photovoltaic (PV) has made striking growth over the past decades due to meagre non-renewable energy resources. The emerging thin film PV technology has the potential for reducing module cost due to less consumption of semiconductor material. Among thin film materials, CIGS is reckoned to be promising absorber material for large area PV applications. CIGS is a semiconductor material having tunable direct bandgap (1.04–1.68 eV) [1] and high absorption coefficient (10^5/cm) in wide absorbing spectrum [2]. In addition, CIGS solar cells have shown high radiation stability [3] with PV conversion efficiency of 21.7% [4].

Vacuum deposition techniques such as co-evaporation [5] and sputtering [6] are well known for obtaining device quality CIGS thin films. However, vacuum based deposition methods have difficulties owing to soaring process cost [7], process complexity, problems in scale up of vacuum equipment and material wastage [8,3]. Developing non-vacuum techniques to obtain device quality CIGS thin films

* Corresponding author at: Department of Electrical Engineering (SEES), CINVESTAV-IPN, Avenida IPN 2508, San Pedro Zacatenco, Mexico D.F., Mexico. Tel.: +52 55 57473800.
E-mail address: velu@cinvestav.mx (S. Velumani).

http://dx.doi.org/10.1016/j.mssp.2015.02.046
1369-8001/

can be a key to overcome the limitations of vacuum methods. Non-vacuum techniques are broadly classified into molecular precursor approach including electrodeposition, spray pyrolysis and nanoparticle approach [9]. Nanoparticle approach involves synthesis and deposition of nanoparticle based precursor material onto a substrate using cost effective simple methods such as spin coating [10], spraying [11], screen printing [12] and doctor blade [13]. Nanoparticle approach is regarded as a feasible method due to good control over atomic concentrations [13], high material usage and simplicity in scale up [3].

There is plethora of chemical methods including a colloidal process [14], solvothermal process [15] and hot injection [16] to synthesize CIGS nanoparticles. But the chemical processes are either time consuming or requires schlenk-line techniques [17]. The mechanochemical process is a powder processing technique, which involves milling powders of metals, alloy or compounds together. During this process material transfer will take place to acquire homogenous alloy [18]. Owing to the potential to have mass production of nanoparticles from non-toxic precursor materials with high energy efficiency in short processing time makes the mechanochemical process a favourable technique to synthesize CIGS nanostructures [2]. Despite this fact, the mechanochemical process is an intricate process. It involves various parameters, such as ball to powder ratio (BPR), milling time and milling speed (rpm) which needs to be optimised to synthesize nanoparticles of desired properties.

Several groups have reported synthesis of CIGS nanoparticle by the mechanochemical process [19–21]. The structural studies of mechanically alloyed CIGS nanoparticles from elemental Cu, In, Ga and Se have been reported by Benslim et al. [19]. The role of milling time on material phase formation and crystallite size of CIGS nanoparticles is recently reported by Rehani [20]. Fu et al. have reported that increased rotational speed is beneficial for pure CIGS formation [21]. In the present work, we synthesized CIGS nanoparticles by the mechanochemical process from elemental precursor materials and studied the importance of milling time, milling speed and BPR on single phase CIGS nanoparticle formation with reduced agglomeration and desired composition. To the best of our knowledge the importance of BPR on mechanochemical synthesis of CIGS is not well investigated. We observed that higher BPR helps to reduce milling time required for the formation of single phase CIGS. Morphology and composition of the mechanochemically synthesized CIGS nanoparticles were also influenced by BPR.

2. Experimental details

The precursor materials used in this work were elemental copper granules (> 99.90 pure, Aldrich), gallium granules (> 99.99 pure, Aldrich), powders of indium (> 99.99 pure, Aldrich) and selenium (> 99.99 pure, Aldrich). The raw material mixture, Cu (0.9408 g), In (0.8495 g), Ga (0.5158 g) and Se (2.3370 g), was taken in a tungsten carbide vial. A planetary ball mill (PM 400, Retsch, Germany) was used with the tungsten carbide vial. Tungsten carbide balls weighing 7.738 g and 10 mm diameter were used as milling media. The reaction undergone in a ball milling process is as follows:

$$Cu + 0.5In + 0.5Ga + 2Se \rightarrow Cu(In, Ga)_{0.5}Se_2 \quad (1)$$

Table 1
Experimental design of the mechanochemical process.

Experimental number	Ball to powder ratio (BPR)	Milling time (h)	Milling speed (rpm)
1	15:1	2	400
2	20:1	2	400
3	25:1	2	400
4	25:1	1	400
5	25:1	6	400
6	25:1	2	200
7	25:1	2	250
8	25:1	2	300
9	25:1	2	350

In order to study the effect of milling time, milling speed and BPR on the reaction, the milling parameters were varied systematically (Table 1). To start with, a BPR of 15:1 was selected while the other parameters such as milling time and milling speed were fixed at 2 h and 400 rpm respectively. Eventually, the BPR was increased to 20:1 and further to 25:1 to find out the minimum BPR for synthesizing single phase CIGS in 2 h. Subsequently, the effect of milling duration was investigated by varying time from 1 to 6 h. Eventually, the effect of milling speed on structural, morphological and compositional properties was studied by varying speed from 200 to 400 rpm with an interval of 50.

X-ray powder diffraction (XRD) analysis performed on a Smart Lab Diffractometer (Rigaku) using Cu Kα radiation ($\lambda = 1.504$ Å) was the main tool used to confirm the formation of CIGS as well as binary compounds. Measured diffraction intensity was in the 2θ range between 20° and 90° with a step size of 0.02° for 6 s per point. Dependence of structural properties of mechanochemically synthesized sample on milling parameter was also deduced from the XRD spectrum. Morphology of the CIGS nanoparticles was analysed using Carl Zeiss Auriga Field emission scanning electron microscopy (FESEM). Composition of the CIGS nanoparticle was analysed by Bruker Ser 5010 X flash Scanning electron microscopy (SEM)-energy dispersive X-ray analysis (EDAX). JEM-ARM200F High resolution transmission electron microscopy (HRTEM) was used to analyse the lattice structure of CIGS.

3. Results and discussion

3.1. Effect of ball to powder ratio

BPR was the first process variable of milling to be investigated. In general higher BPR shortens the milling time required to form single phase of desired material [22]. The BPR was initially set as 15:1 whilst other parameters such as milling time and milling speed were kept as 2 h and 400 rpm respectively. The XRD results of samples as a function of BPR is shown in Fig. 1. It was observed that single chalcopyrite phase CIGS formation took place at BPR of 25:1. The sample obtained with 15:1

Please cite this article as: M. Rohini, et al., Materials Science in Semiconductor Processing (2015), http://dx.doi.org/10.1016/j.mssp.2015.02.046

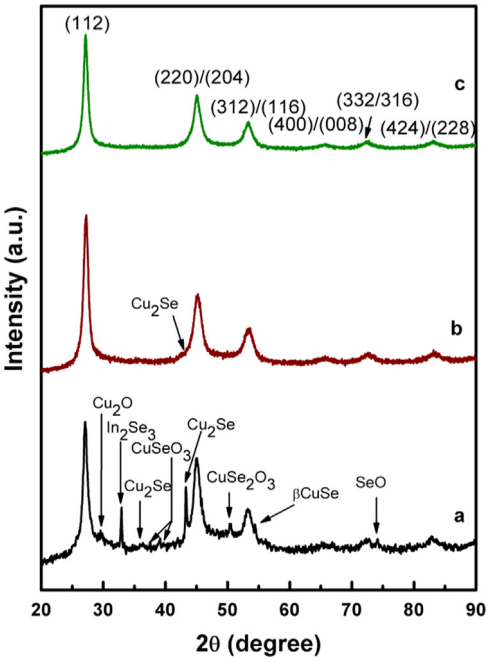

Fig. 1. XRD pattern of CIGS samples milled for 2 h with different BPR (a) 15:1, (b) 20:1 and (c) 25:1.

BPR showed peaks corresponding to both chalcopyrite phases and secondary phases (Fig. 1(a)). The presence of peaks at 2θ corresponding to (112), (220)/(204) and (312)/(116) planes of CIGS in Fig. 1(a) indicated that CIGS phase formation took place at 15:1 BPR in 2 h. The small intensity peaks observed in Fig. 1(a) at 2θ=29.64°, 32.8°, 36.38°, 37.56°, 39.14°, 43.68°, 50.34°, 54.4° and 74.16° related to binary phases Cu_2O, In_2Se_3, αCu_2Se, $CuSeO_3$, βCu_2Se, $CuSe_2O_3$, $\beta CuSe$ and SeO respectively. Subsequently, as the BPR was increased to 20:1, the number of peaks corresponding to secondary phases reduced (Fig. 1(b)). A small intensity peak pointing Cu_2Se was observed. It showed necessity of increasing milling time to form single phase CIGS with BPR of 15:1 and 20:1. A further increase in BPR to 25:1 resulted in a complete reaction in 2 h which was evidenced by the presence of peaks related to single phase of CIGS without any binary phases (Fig. 1(c)). The results emphasised that with increasing BPR, CIGS formation took place in shorter milling time. It was due to the fact that higher energy was supplied to the milled powders at higher BPR. Thus activation energy for the formation of CIGS was provided in 2 h at 25:1 BPR. However, 2 h was not sufficient for single phase CIGS formation with BPR of 15:1 and 20:1 due to insufficient supply of energy [22].

The FESEM images of mechanochemically synthesized samples with BPR of 15:1, 20:1 and 25:1 for 2 h are shown in Fig. 2(a)–(c) respectively. Fig. 2(a) showed highly cold welded agglomerates of CIGS nanostructures. We could observe individual and agglomerated spherical structures over the large cold welded structure. Fig. 2(b) exhibited cold welded structure which is smaller as compared to that in Fig. 2(a). It could be assumed as broken part of structures observed in Fig. 2(a). Large number of smaller

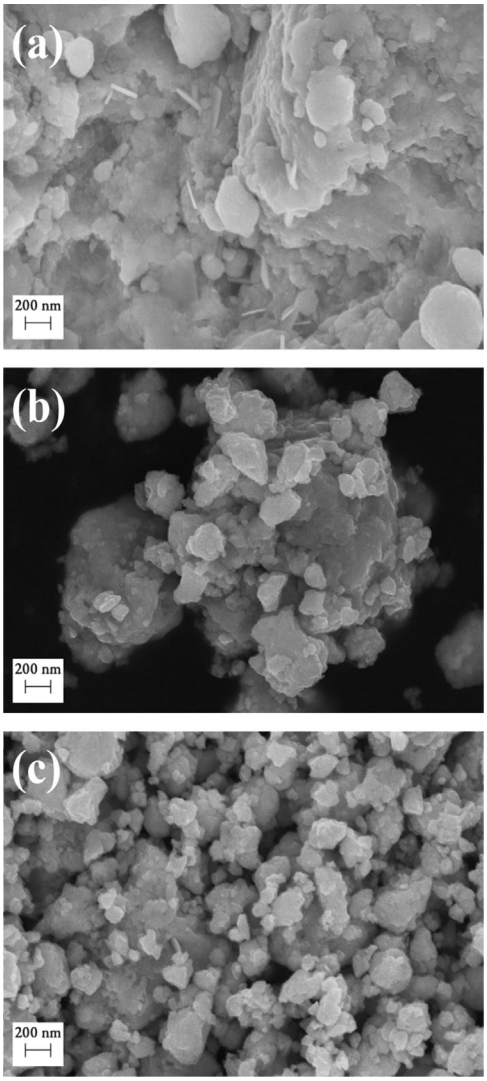

Fig. 2. FESEM images of CIGS samples milled for 2 h with different BPR (a) 15:1, (b) 20:1 and (c) 25:1.

spherical structures was observed in Fig. 2(c) relative to Fig. 2(a) and (b). It proclaimed the dependence of morphology of nanostructures on BPR. As BPR increased, total number of balls increased. Hence the frequency of collisions rose and mean free path between two collisions declined. Thereby energy input to the process increased [18]. Thus, the time span between different stages such as cold welding, fracturing and rewelding in milling will be less, so that the products obtained at higher BPR will be smaller and less agglomerated.

The results of EDAX analysis are given in Table 2. The results showed the influence of BPR on determining composition of final product. Atomic percentage of Cu was found to rise from 24.01 to 27.32 with increasing BPR from 15:1 to 20:1 while Se atomic percentage decreased from 52.49 to 48.89. Whereas an increase in atomic percentage of In was observed with changing BPR from 20:1 to 25:1.The results indicated that higher BPR favours incorporation of Cu and In, whilst it would lead to loss of

Please cite this article as: M. Rohini, et al., Materials Science in Semiconductor Processing (2015), http://dx.doi.org/10.1016/j.mssp.2015.02.046

Table 2
EDAX data of CIGS samples milled with different BPRs.

BPR	Atomic percentage of elements (%)				Ga/In+Ga	Cu/In+Ga
	Cu	In	Ga	Se		
15:1	24.01	10.08	13.42	52.49	0.57	1.02
20:1	27.32	10.46	13.33	48.89	0.56	1.15
25:1	27.55	11.40	12.65	48.40	0.52	1.14

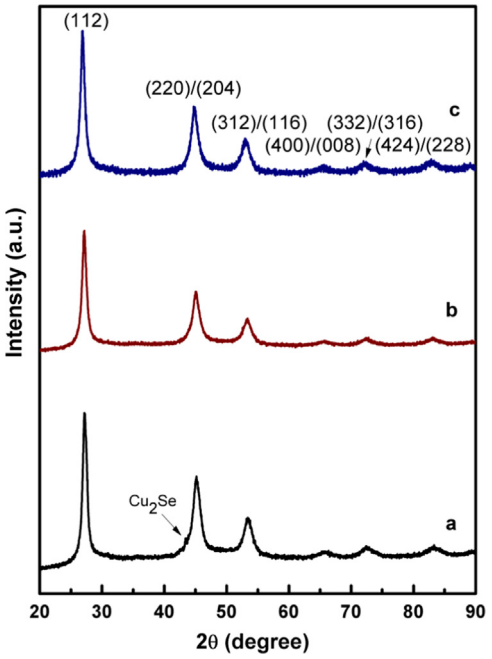

Fig. 3. XRD pattern of CIGS samples milled with BPR of 25:1 for different milling times: (a) 1 h, (b) 2 h and (c) 6 h.

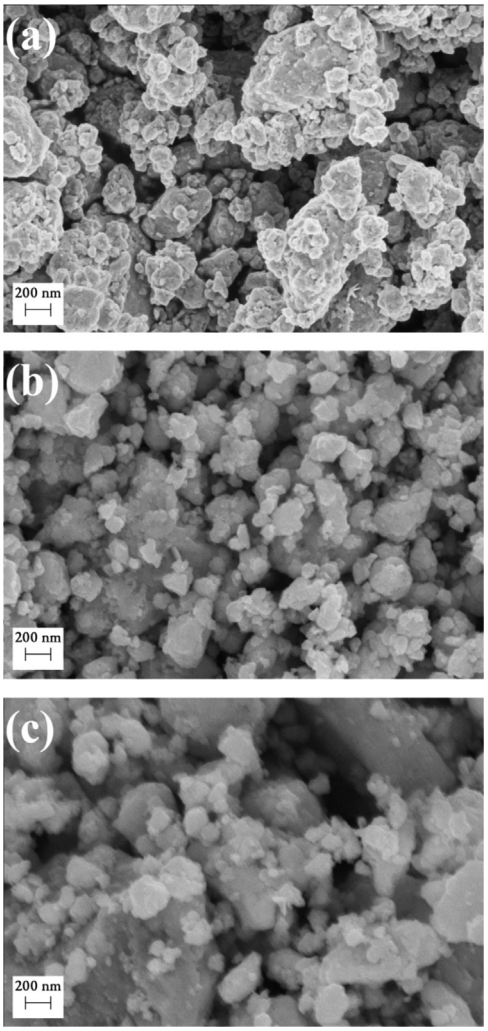

Fig. 4. FESEM images of CIGS samples milled with BPR of 25:1 for different milling times: (a) 1 h, (b) 2 h and (c) 6 h.

Se due to higher heat energy developed with high BPR. The sample milled with 25:1 showed Ga/In+Ga closely matching to the initial precursor stoichiometry $Cu(In,Ga)_{0.5}Se_2$. As single phase, less agglomerated and stoichiometric CIGS nanoparticles were obtained with BPR of 25:1, we fixed 25:1 as optimum BPR for further experiments.

3.2. *Effect of milling time*

The milling time is a significant milling parameter. The time required to form single phase CIGS will be determined by type of mill, milling settings, and intensity of milling [23]. We had varied milling time from 1 to 6 h whereas milling speed was maintained as 400 rpm. The experiments were carried out keeping BPR as 25:1 as single phase chalcopyrite formation took place with BPR of 25:1 in 2 h.

The XRD of CIGS powder obtained by milling for 1, 2 and 6 h are shown in Fig. 3. All the samples showed diffracted peaks associated to chalcopyrite phases of CIGS. A small intensity shoulder peak on (220)/(204) and a prominent peak corresponding to (371) plane of Cu_2Se was observed (JCPDS 47-1448). The presence of binary phase in the sample milled for 1 h demonstrated that 2 h is the minimum time required to form single phase CIGS with BPR of 25:1 at 400 rpm.

Fig. 4 showed FESEM micrograph of CIGS nanoparticles milled for 1, 2 and 6 h. Solid agglomerated structures were observed in 1 h milled sample. Whilst smaller spherical like structures were observed in sample milled for 2 h along with flat big agglomerated structures. Nevertheless, highly agglomerated structures were found after milling for 6 h. The tendency of agglomeration increases as fractured particles gained high surface energy. High surface energy and cohesion among particles with decreasing particle size account for agglomeration. The fracturing and cold welding mechanisms continue as milling time prolongs [24]. Hence optimization of milling time is necessary to obtain less agglomerated nanostructures by the mechanochemical process.

EDAX analysis showed that atomic percentage of Cu increased with milling time (Table 3) while Se atomic percentage decreased. This was in accordance with the results reported by Vidya et al. [25]. Loss of Se at higher milling time may be due to volatilization with increased

Please cite this article as: M. Rohini, et al., Materials Science in Semiconductor Processing (2015), http://dx.doi.org/10.1016/j.mssp.2015.02.046

Table 3
EDAX data of CIGS samples milled for different milling times.

Milling time (h)	Atomic percentage of elements (%)				Ga/In+Ga	Cu/In+Ga
	Cu	In	Ga	Se		
1	25.74	12.53	12.97	48.76	0.51	1.01
2	27.55	11.40	12.65	48.40	0.52	1.14
6	28.24	11.16	12.65	47.95	0.53	1.20

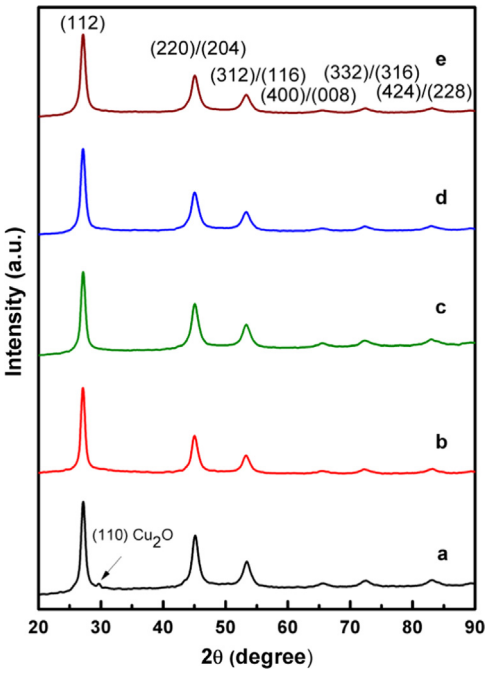

Fig. 5. XRD pattern of CIGS samples milled for 2 h with BPR of 25:1 at different milling speeds: (a) 200, (b) 250, (c) 300, (d) 350 and (e) 400 rpm.

temperature inside the vial as milling time increases. The results emphasised the importance of milling time to obtain stoichiometric CIGS nanoparticles. As 2 h was the minimum time required to synthesize single phase CIGS nanoparticles with less agglomeration, 2 h was considered to be the optimum milling time for further experiments.

3.3. *Effect of milling speed*

XRD pattern of CIGS powder after mechanochemical synthesis for 2 h with BPR of 25:1 at 200, 250, 300, 350 and 400 rpm are shown in Fig. 5. All samples showed diffraction peaks related to (112), (220)/(204) and (312)/(116) planes of chalcopyrite phase. Broad and sharp peaks indicated the nanocrystalline nature of mechanochemically synthesized CIGS powder. A low intensity peak observed at 30° designates the presence of Cu_2O phase in the sample milled at 200 rpm. The Cu_2O phase disappeared when the milling speed reached 250 rpm. It revealed that increasing milling speed is favourable for the incorporation of Cu and formation of single phase CIGS. It might be due to the fact that increasing milling speed provides higher energy which drives the chemical reaction among Cu, In, Ga and Se to form pure phase of CIGS [21].

FESEM images of CIGS nanoparticles obtained after milling for 2 h with BPR of 25:1 at 200, 250, 300, 350 and 400 rpm are shown in Fig. 6. The sample obtained with 200 rpm showed spherical and plate like structures. The plate like structures could be due to flattening of materials during milling. The structures were strongly welded. CIGS nanoparticles milled with 250, 300 and 350 rpm showed similar morphology. Relative to Fig. 6(c), size of cold welded grains were found to be larger in Fig. 6(d). Disappearance of plate like structures was observed with increasing milling speed. Sample milled with 400 rpm showed more defined spherical particles along with bigger aggregates of cold welded grains.

The EDAX composition analysis (Table 4) showed difference in ratio of Ga/In+Ga and Cu/In+Ga with changing milling speed. A non-linear variation in atomic percentage of In with milling speed varying from 200 to 300 rpm could be due to non-homogenous distribution of elements in the sample. Increasing milling speed seemed to have no effect on controlling atomic percentage of Cu and Se as compared to milling time and BPR while an increase in atomic percentage of In and decreasing atomic percentages of Ga were observed with increasing milling speed.

3.4. *Mechanism of CIGS nanoparticle synthesis by mechanochemical process*

Wada et.al reported that mechanochemical synthesis of CIS is a self-propagating high temperature synthesis (SHS) in which the reaction gets started by the mechanical energy transferred to the reactant material from the collisions and frictions with the balls used in the milling process [26]. The initiation of Cu+In+Ga+2Se reaction by mechanical energy could be explained on the basis of thermochemical data. The minimum adiabatic temperature (T_{ad}) needed for initiating a SHS reaction is reported as 1800 K or $[\Delta H/C_p]298\ K = 2000\ K$. But, due to the welding and fracture mechanism occurring in the mechanochemical process the interfacial area of the reactants will increase. This resulted in exposure of clean surfaces and increase in defect density which helps the reactants to diffuse along the defects so that the T_{ad} will decrease to 1300 K from 2000 K [27]. The reported values of molar heat capacity, $C_{p(298.15\ K)}$, of CIS and CGS are 99.82 J/mol K and 98.16 J/mol K respectively [28,29]. The calculated values for enthalpy of formation for CIS and CGS were obtained from literatures as ΔH_f (CIS) = −218.50 kJ/mol and ΔH_f (CGS) = −251 kJ/mol [27,30]. Hence, the adiabatic temperature of reaction (T_{ad}) is calculated as, $[\Delta H/C_p]_{298\ K} = 2188.94$ K for CIS and 2557.05 K for CGS. Thus, T_{ad} for the reaction of CIGS formation will be in between 2188.94 K and 2557.04 K (depending on the Ga concentration), which is much larger than 1300 K. Hence, the mechanochemical synthesis of CIGS could take place easily. In our experiments, we obtained single phase CIGS in 2 h of milling using BPR of 25:1 at a milling speed of 400 rpm. HRTEM images of the CIGS nanoparticles obtained at the above mentioned milling conditions are

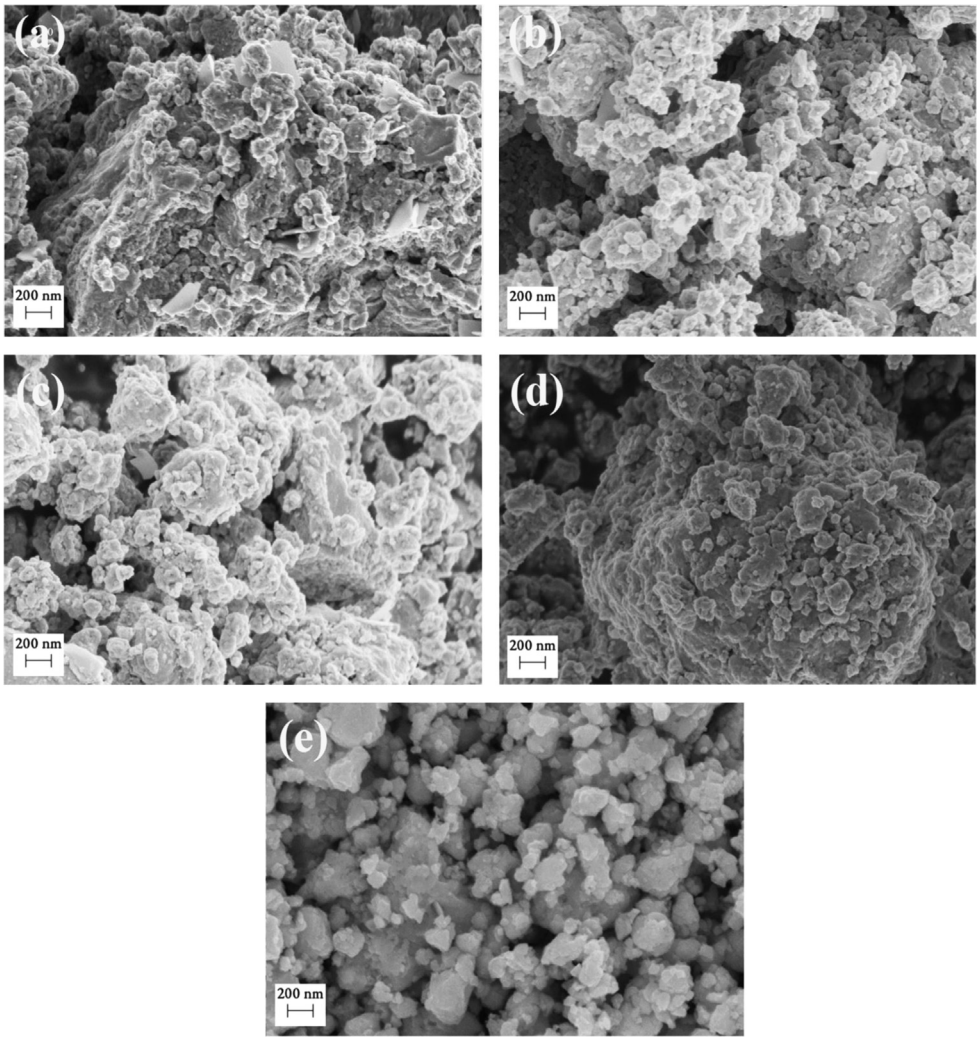

Fig. 6. FESEM images of CIGS samples milled for 2 h with BPR of 25:1 at different milling speeds: (a) 200, (b) 250, (c) 300, (d) 350 and (e) 400 rpm.

Table 4
EDAX data of CIGS samples milled with different milling speeds.

Milling speed (rpm)	Atomic percentage of elements (%)				Ga/In+Ga	Cu/In+Ga
	Cu	In	Ga	Se		
200	27.23	10.42	13.99	48.36	0.57	1.11
250	27.94	9.90	13.15	49.01	0.57	1.21
300	27.47	10.84	12.93	48.76	0.54	1.15
350	28.04	11.54	12.71	47.71	0.52	1.16
400	27.55	11.40	12.65	48.40	0.52	1.14

shown in Fig. 7. It was observed from Fig. 7(a) that the sample consisted of strongly aggregated CIGS nanoparticles, but the crystallite size of individual particle was 17 nm as depicted from Fig. 7(b). High degree of crystallinity was observed from HRTEM image (Fig. 7(c)). Lattice spacing of planes were found from HRTEM and FFT of HRTEM (Fig. 7(c), and (d)). They were in consistent with the chalcopyrite structure (JCPDS-40-1488). The observed loss of Se with higher BPR and milling time could be due to vaporization of Se as heat of vaporization of Se is small (26.3 kJ/mol) [25]. This was evidenced by the presence of Se in oxide form on the lid of the container.

4. Conclusion

In this study, $Cu(In,Ga)_{0.5}Se_2$ nanoparticles were synthesized by the mechanochemical process. We investigated the effect of BPR, milling time and milling speed on the formation of less agglomerated single phase CIGS nanoparticles with desired composition. It was found that at a fixed milling time of 2 h and milling speed of 400 rpm, higher BPR favours single phase CIGS formation compared to that of lower BPR. Agglomeration of nanostructures got increased with increasing milling time while less agglomerated nanostructures were formed by increasing BPR and milling speed. Higher BPR and milling time were found to be beneficial for increasing atomic percentages of Cu and In while no significant increase in atomic percentage of Cu was observed with increasing milling speed. Atomic percentage of Se was found to decrease at higher BPR and

Please cite this article as: M. Rohini, et al., Materials Science in Semiconductor Processing (2015), http://dx.doi.org/10.1016/j.mssp.2015.02.046

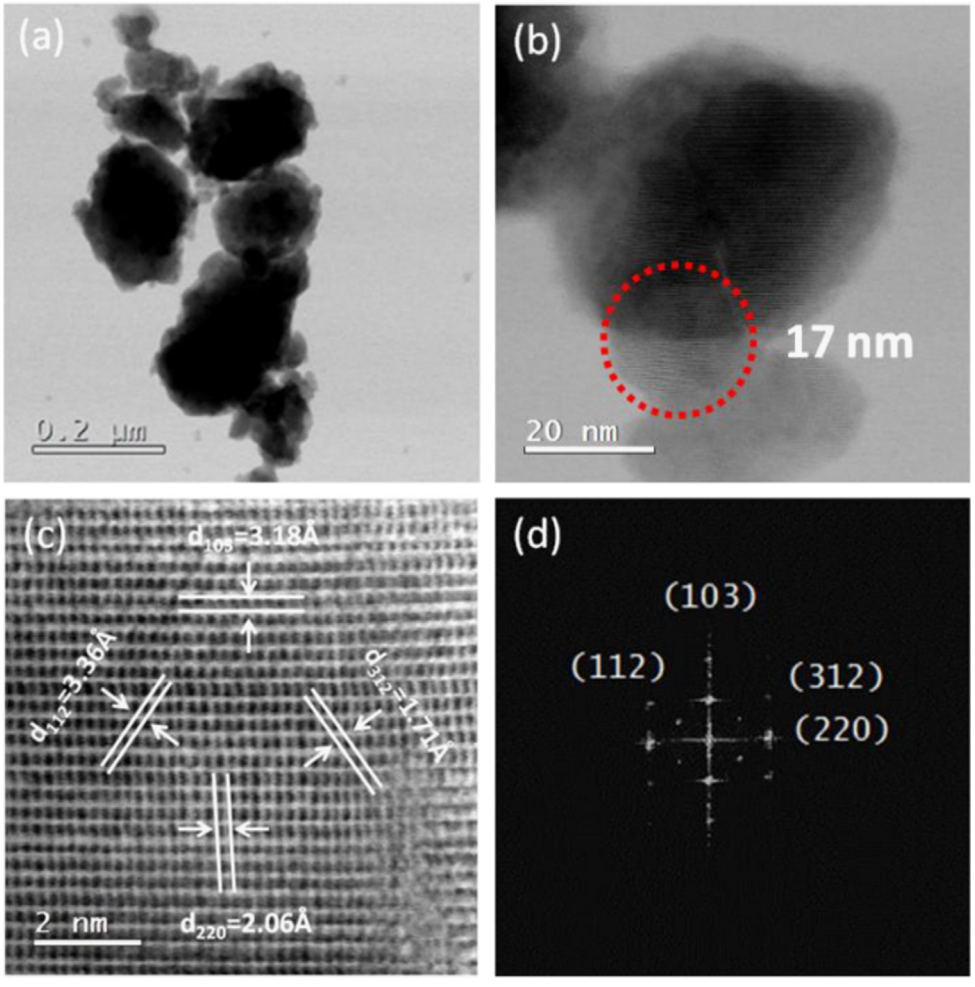

Fig. 7. (a) TEM image (b, c) HRTEM images (d) its FFT of CIGS samples milled at BPR of 25:1 at 400 rpm for 2 h.

higher milling time. The mechanochemically synthesized CIGS nanoparticles will be used for deposition of thin films for solar cell applications.

Acknowledgements

Authors acknowledge the partial financial support from the project CeMIE-Sol 207450/P26. Also, we would like to acknowledge Marcela Guerrero for her help in XRD measurement. We also acknowledge J.E.Romero-Ibarra and Alvaro Angeles Pascual for their technical help in FESEM, EDAX and HRTEM analyses.

References

[1] C.H. Lu, C.H. Lee, C.H. Wu, Sol. Energy Mater. Sol. Cells 94 (2010) 1622–1626.
[2] B. Vidya, S. Velumani, A. Jesus., A. Alatorre, A.M. Acevedo, R. Asomoza, J.A.C. Carvayar, Mater. Sci. Eng. B 174 (2010) 216–222.
[3] Y. Liu, D. Kong, H. You, C. Zhao, J. Li, Electrochem. Solid-State Lett. 1 (2012) 26–28.
[4] Press release dated 22nd September. ⟨http://www.pv-magazine.com/news/details/beitrag/zsw-sets-217-thin-film-efficiency-record_100016505/axzz3IAXN9AUl⟩, 2014 (accessed 24.11.14).
[5] T. Wada, H. Kinoshita, S. Kawata, Thin Solid Films 431–432 (2003) 11–15.
[6] K. Ramanathan, M.A. Contreras, C.L. Perkins, S. Asher, F.S. Hasoon, Prog. Photovolt. Res. Appl. 11 (2003) 225–230.
[7] J. liu, D. Zhuang, H. Luan, M. Cao, M. Xie, Prog. Nat. Sci. 23 (2013) 133–138.
[8] C. Eberspacher, C. Fredric, K. Pauls, J. Serra, Thin Solid Films. 387 (2001) 18–22.
[9] D. Lee, K. Yong, Korean J. Chem. Eng. 30 (2013) 1347–1358.
[10] Y. Liu, D. Kong, J Li, C. Zhao, C. Chen, J. Brugger, Energy Procedia 16 (2012) 217–222.
[11] J.A. Hollingsworth, K.K. Banger, M.H.-C. Jin, J.D. Harris, J.E. Cowen, E.W. Bohannan, J.A. Switzer, W.E. Buhro, A.F. Hepp, Thin Solid Films 431–432 (2003) 63–67.
[12] M. Kaelin, H. Zogg, A.N. Tiwari, O. Wilhelm, S.E. Pratsinis, T. Meyer, A. Meyer, Thin Solid Films 457 (2004) 391–396.
[13] S.R. Dhage, M. Tak, S.V. Joshi, Mater. Lett. 134 (2014) 302–305.
[14] W.H. Hsu, H.I. Hsiang, F.C. Yen, S.C. Shei, F.S. Yen, J. Eur. Ceram. Soc. 32 (2012) 3753–3757.
[15] Y.G Chun, K.H. Kim, K.H. Yoon, Thin Solid Films 480/481 (2005) 46–49.
[16] D.C. Nguyen, K. Fukatsu, K. Tanimoto, S. Ikeda, M. Matsumura, S. Ito, Int. J. Photoenergy 2013 (2013) 1–7.
[17] Y. Liu, D. Kong, H. You, C. Zhao, J. Li, J. Brugger, Electrochem. Solid-State Lett. 1 (2012) 26–28.
[18] A. Canakci, F. Erdemir, T. Varol, A. Patir, Measurement 46 (2013) 3532–3540.
[19] N. Benslim, S. Mehdaoui, O. Aissaoui, M. Benabdeslem, A. Bouasla, L. Bechiri, A. Otmani, X. Portier, J. Alloy. Compd. 489 (2010) 437–440.

[20] B. Rehani, J.R. Ray, C.J. Panchal, H. Master, R.R. Desai, P.B. Patel, J. Nano-Electron. Phys. 5 (2013) 02007-1–02007-4.
[21] L. Fu, Y.Q. Guo, S. Zheng, Powder Diffr. 28 (2013) 1–3.
[22] M. Zakeria, M. Ramezanib, A. Nazaric, Mater. Res. 15 (2012) 891–897.
[23] C. Suryanarayana, Prog. Mater. Sci. 46 (2001) 1–184.
[24] H. Zuhailawati, Y. Mahani, J. Alloy. Compd. 476 (2009) 142–146.
[25] B Vidhya, S. Velumani, R. Asomoza, J. Nanoparticle Res. 13 (2011) 3033–3042.
[26] T. Wada, H. Kinoshita, J. Phys. Chem. Solids 66 (2005) 1987–1989.
[27] S Wu, Y. Xue, Z. Zhang, J. Alloy. Compd. 491 (2010) 456–459.
[28] E. Gmelin, W. Hönle, Thermichim. Acta 269/270 (1995) 575–590.
[29] J. Bischof, K. Bohmhammel, P. Deus, Cryst. Res. Technol. 23 (1988) 543–548.
[30] A. Jäger-Waldau, N. Meyer, T. Weiss, S. Fiechter, M. Ch.Lux-Steiner, K. Tempelhoff, W. Richter, Jpn. J. Appl. Phys. 37 (1998) 1617–1621.

Please cite this article as: M. Rohini, et al., Materials Science in Semiconductor Processing (2015), http://dx.doi.org/10.1016/j.mssp.2015.02.046